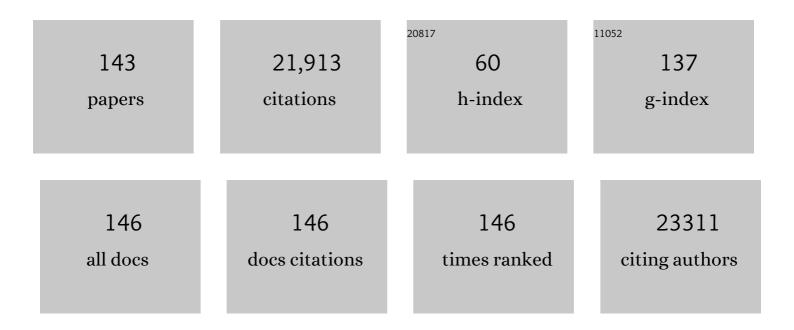
List of Publications by Year in descending order

Source: https://exaly.com/author-pdf/7323720/publications.pdf Version: 2024-02-01



#	Article	IF	CITATIONS
1	Electronic Coupling of Single Atom and FePS <sub>3</sub> Boosts Water Electrolysis. Energy and Environmental Materials, 2022, 5, 899-905.	12.8	16
2	Utilizing tannic acid and polypyrrle to induce reconstruction to optimize the activity of MOF-derived electrocatalyst for water oxidation in seawater. Chemical Engineering Journal, 2022, 430, 132632.	12.7	15
3	Photocatalyst with Chloroplastâ€like Structure for Enhancing Hydrogen Evolution Reaction. Energy and Environmental Materials, 2022, 5, 1229-1237.	12.8	15
4	Porous hard carbon spheres derived from biomass for high-performance sodium/potassium-ion batteries. Nanotechnology, 2022, 33, 055401.	2.6	23
5	Surfactant-free self-assembled MXene/carbon nanotubes hybrids for high-rate sodium- and potassium-ion storage. Journal of Alloys and Compounds, 2022, 901, 163426.	5.5	16
6	Self-assembled transition metal chalcogenides@CoAl-LDH 2D/2D heterostructures with enhanced photoactivity for hydrogen evolution. Inorganic Chemistry Frontiers, 2022, 9, 994-1005.	6.0	13
7	Room-Temperature Assembled MXene-Based Aerogels for High Mass-Loading Sodium-Ion Storage. Nano-Micro Letters, 2022, 14, 37.	27.0	49
8	Highly efficient oxygen evolution catalysis achieved by NiFe oxyhydroxide clusters anchored on carbon black. Journal of Materials Chemistry A, 2022, 10, 10342-10349.	10.3	13
9	Stabilizing BiOCl/Ti <sub>3</sub> C <sub>2</sub> T <sub><i>x</i></sub> hybrids for potassium-ion batteries <i>via</i> solid electrolyte interphase reconstruction. Inorganic Chemistry Frontiers, 2022, 9, 3165-3175.	6.0	5
10	Multifunctional Sensors Based on Doped Indium Oxide Nanocrystals. ACS Applied Materials & Interfaces, 2022, 14, 24648-24658.	8.0	5
11	Plasma-engineered bifunctional cobalt–metal organic framework derivatives for high-performance complete water electrolysis. Nanoscale, 2021, 13, 6201-6211.	5.6	14
12	Facial synthesis of two-dimensional In <sub>2</sub> S <sub>3</sub> /Ti <sub>3</sub> C <sub>2</sub> T <sub><i>x</i></sub> heterostructures with boosted photoactivity for the hydrogenation of nitroaromatic compounds. Materials Chemistry Frontiers, 2021, 5, 6883-6890.	5.9	9
13	Electrostatically confined Bi/Ti <sub>3</sub> C <sub>2</sub> T <sub><i>x</i></sub> on a sponge as an easily recyclable and durable catalyst for the reductive transformation of nitroarenes. Journal of Materials Chemistry A, 2021, 9, 19847-19853.	10.3	12
14	Selectivity control of organic chemical synthesis over plasmonic metal-based photocatalysts. Catalysis Science and Technology, 2021, 11, 425-443.	4.1	5
15	2D Titanium Carbide (MXene) Based Films: Expanding the Frontier of Functional Film Materials. Advanced Functional Materials, 2021, 31, 2105043.	14.9	50
16	Asymmetric structure engineering of polymeric carbon nitride for visible-light-driven reduction reactions. Nano Energy, 2021, 87, 106168.	16.0	32
17	Achieving Highâ€Performance 3D K <sup>+</sup> â€Preâ€intercalated Ti <sub>3</sub> C <sub>2</sub> T <sub><i>x</i></sub> MXene for Potassiumâ€ion Hybrid Capacitors via Regulating Electrolyte Solvation Structure. Angewandte Chemie, 2021, 133, 26450-26457.	2.0	3
18	Achieving Highâ€Performance 3D K <sup>+</sup> â€Preâ€intercalated Ti <sub>3</sub> C <sub>2</sub> T <sub><i>x</i></sub> MXene for Potassiumâ€ion Hybrid Capacitors via Regulating Electrolyte Solvation Structure. Angewandte Chemie - International Edition, 2021, 60, 26246-26253.	13.8	50

#	Article	IF	CITATIONS
19	The band engineering of 2D-hybridized PCN-Sb <sub>2</sub> MoO <sub>6</sub> -Bi <sub>2</sub> O <sub>3</sub> nanomaterials with dual Z-scheme heterojunction for enhanced photocatalytic water splitting without sacrificial agents. Sustainable Energy and Fuels, 2021, 5, 2325-2334.	4.9	5
20	Schottky Junctions with Bi Cocatalyst for Taming Aqueous Phase N <sub>2</sub> Reduction toward Enhanced Solar Ammonia Production. Advanced Science, 2021, 8, 2003626.	11.2	56
21	Surface Chemistry and Mesopore Dual Regulation by Sulfurâ€Promised High Volumetric Capacity of Ti <sub>3</sub> C <sub>2</sub> T <i><sub>x</sub></i> Films for Sodiumâ€lon Storage. Small, 2021, 17, e2103626.	10.0	19
22	Tip-grafted Ag-ZnO nanorod arrays decorated with Au clusters for enhanced photocatalysis. Catalysis Today, 2020, 340, 121-127.	4.4	31
23	Bi-metallic cobalt-nickel phosphide nanowires for electrocatalysis of the oxygen and hydrogen evolution reactions. Catalysis Today, 2020, 358, 196-202.	4.4	46
24	Robust and easily retrievable Pd/Ti3C2T âŠ,graphene hydrogels for efficient catalytic hydrogenation of nitroaromatic compounds. Chinese Chemical Letters, 2020, 31, 1014-1017.	9.0	35
25	Support interactions dictated active edge sites over MoS <sub>2</sub> –carbon composites for hydrogen evolution. Nanoscale, 2020, 12, 1109-1117.	5.6	23
26	Ultrafine oxygen-defective iridium oxide nanoclusters for efficient and durable water oxidation at high current densities in acidic media. Journal of Materials Chemistry A, 2020, 8, 24743-24751.	10.3	45
27	Rising from the horizon: three-dimensional functional architectures assembled with MXene nanosheets. Journal of Materials Chemistry A, 2020, 8, 18538-18559.	10.3	86
28	Design of novel structured Au/g-C <sub>3</sub> N <sub>4</sub> nanosheet/reduced graphene oxide nanocomposites for enhanced visible light photocatalytic activities. Sustainable Energy and Fuels, 2020, 4, 4086-4095.	4.9	12
29	Facile Fabrication of a Novel Au/Phosphorus-Doped g-C3N4 Photocatalyst with Excellent Visible Light Photocatalytic Activity. Catalysts, 2020, 10, 701.	3.5	15
30	Positioning MXenes in the Photocatalysis Landscape: Competitiveness, Challenges, and Future Perspectives. Advanced Functional Materials, 2020, 30, 2002528.	14.9	162
31	Artificial nitrogen fixation over bismuth-based photocatalysts: fundamentals and future perspectives. Journal of Materials Chemistry A, 2020, 8, 4978-4995.	10.3	97
32	Ultrafine-Grained Porous Ir-Based Catalysts for High-Performance Overall Water Splitting in Acidic Media. ACS Applied Energy Materials, 2020, 3, 3736-3744.	5.1	26
33	A retrospective on MXene-based composites for solar fuel production. Pure and Applied Chemistry, 2020, 92, 1953-1969.	1.9	14
34	Hierarchically tailorable double-array film hybrids with enhanced photocatalytic and photoelectrochemical performances. Applied Catalysis B: Environmental, 2019, 259, 118086.	20.2	15
35	Horizons Community Board collection – emerging 2D materials for energy and electronics applications. Materials Horizons, 2019, 6, 1092-1093.	12.2	0
36	Nitrogen-doped Carbon with Modulated Surface Chemistry and Porous Structure by a Stepwise Biomass Activation Process towards Enhanced Electrochemical Lithium-Ion Storage. Scientific Reports, 2019, 9, 15032.	3.3	24

#	Article	IF	CITATIONS
37	Microstructure and surface control of MXene films for water purification. Nature Sustainability, 2019, 2, 856-862.	23.7	273
38	Horizons Community Board collection – emerging 2D materials for energy and electronics applications. Nanoscale Horizons, 2019, 4, 1027-1028.	8.0	1
39	Broadband Light Harvesting and Unidirectional Electron Flow for Efficient Electron Accumulation for Hydrogen Generation. Angewandte Chemie, 2019, 131, 10108-10112.	2.0	17
40	Broadband Light Harvesting and Unidirectional Electron Flow for Efficient Electron Accumulation for Hydrogen Generation. Angewandte Chemie - International Edition, 2019, 58, 10003-10007.	13.8	86
41	Toward rational algorithmic design of collagen-based biomaterials through multiscale computational modeling. Current Opinion in Chemical Engineering, 2019, 24, 79-87.	7.8	13
42	Chemical ordering and relaxor properties in a novel solid solution of (1-x)Pb(Mg1/3Nb2/3)O3-xPb(Cd1/3Nb2/3)O3. Ferroelectrics, 2019, 553, 14-25.	0.6	0
43	3D graphene/AgBr/Ag cascade aerogel for efficient photocatalytic disinfection. Applied Catalysis B: Environmental, 2019, 245, 343-350.	20.2	87
44	Photoredox catalysis over graphene aerogel-supported composites. Journal of Materials Chemistry A, 2018, 6, 4590-4604.	10.3	171
45	Eu and F co-doped ZnO-based transparent electrodes for organic and quantum dot light-emitting diodes. Journal of Materials Chemistry C, 2018, 6, 5542-5551.	5.5	14
46	Mesoporous Hybrid Electrolyte for Simultaneously Inhibiting Lithium Dendrites and Polysulfide Shuttle in Li–S Batteries. Advanced Energy Materials, 2018, 8, 1703124.	19.5	42
47	WO <sub>3</sub> â€Based Electrochromic Distributed Bragg Reflector: Toward Electrically Tunable Microcavity Luminescent Device. Advanced Optical Materials, 2018, 6, 1700791.	7.3	45
48	Hollow cobalt phosphide octahedral pre-catalysts with exceptionally high intrinsic catalytic activity for electro-oxidation of water and methanol. Journal of Materials Chemistry A, 2018, 6, 20646-20652.	10.3	95
49	An adaptive geometry regulation strategy for 3D graphene materials: towards advanced hybrid photocatalysts. Chemical Science, 2018, 9, 8876-8882.	7.4	29
50	Dynamic Migration of Surface Fluorine Anions on Cobaltâ€Based Materials to Achieve Enhanced Oxygen Evolution Catalysis. Angewandte Chemie, 2018, 130, 15697-15701.	2.0	11
51	Dynamic Migration of Surface Fluorine Anions on Cobaltâ€Based Materials to Achieve Enhanced Oxygen Evolution Catalysis. Angewandte Chemie - International Edition, 2018, 57, 15471-15475.	13.8	178
52	Ti3C2Tx MXene as a Janus cocatalyst for concurrent promoted photoactivity and inhibited photocorrosion. Applied Catalysis B: Environmental, 2018, 237, 43-49.	20.2	174
53	Function-Oriented Engineering of Metal-Based Nanohybrids for Photoredox Catalysis: Exerting Plasmonic Effect and Beyond. CheM, 2018, 4, 1832-1861.	11.7	147
54	Light-tuned switching of charge transfer channel for simultaneously boosted photoactivity and stability. Applied Catalysis B: Environmental, 2018, 238, 19-26.	20.2	48

#	Article	IF	CITATIONS
55	Advances in materials engineering of CdS coupled with dual cocatalysts of graphene and MoS <sub>2</sub> for photocatalytic hydrogen evolution. Pure and Applied Chemistry, 2018, 90, 1379-1392.	1.9	4
56	Enhanced Performance and Flexibility of Perovskite Solar Cells Based on Microstructured Multilayer Transparent Electrodes. ACS Applied Materials & Interfaces, 2018, 10, 18141-18148.	8.0	23
57	Stressâ€Transferâ€Induced Inâ€Situ Formation of Ultrathin Nickel Phosphide Nanosheets for Efficient Hydrogen Evolution. Angewandte Chemie, 2018, 130, 13266-13269.	2.0	26
58	Stressâ€Transferâ€Induced Inâ€Situ Formation of Ultrathin Nickel Phosphide Nanosheets for Efficient Hydrogen Evolution. Angewandte Chemie - International Edition, 2018, 57, 13082-13085.	13.8	97
59	Study on the Photoresponse Characteristics of Organic Light-Emitting Field-Effect Transistors. Journal of Physical Chemistry C, 2018, 122, 15190-15197.	3.1	1
60	Determination of chemical ordering in the complex perovskite Pb(Cd <sub>1/3</sub> Nb <sub>2/3</sub> )O <sub>3</sub> . IUCrJ, 2018, 5, 808-815.	2.2	5
61	Structure buckling hybrid reliability analysis of a supercavitating projectile using a model with truncated probability and multi-ellipsoid convex set uncertainties. Mechanics Based Design of Structures and Machines, 2017, 45, 173-189.	4.7	2
62	Graphene and its derivatives as versatile templates for materials synthesis and functional applications. Nanoscale, 2017, 9, 2398-2416.	5.6	121
63	Electrocatalysis for the oxygen evolution reaction: recent development and future perspectives. Chemical Society Reviews, 2017, 46, 337-365.	38.1	4,505
64	Sb2O3/Ag/Sb2O3 Multilayer Transparent Conducting Films For Ultraviolet Organic Light-emitting Diode. Scientific Reports, 2017, 7, 41250.	3.3	35
65	Aluminumâ€Based Plasmonic Photocatalysis. Particle and Particle Systems Characterization, 2017, 34, 1600357.	2.3	46
66	Metal-free, robust, and regenerable 3D graphene–organics aerogel with high and stable photosensitization efficiency. Journal of Catalysis, 2017, 346, 21-29.	6.2	86
67	Insight into the Role of Size Modulation on Tuning the Band Gap and Photocatalytic Performance of Semiconducting Nitrogen-Doped Graphene. Langmuir, 2017, 33, 3161-3169.	3.5	36
68	Near-Infrared to Visible Organic Upconversion Devices Based on Organic Light-Emitting Field Effect Transistors. ACS Applied Materials & Interfaces, 2017, 9, 36103-36110.	8.0	26
69	Blue Quantum Dot Light-Emitting Diodes with High Electroluminescent Efficiency. ACS Applied Materials & Interfaces, 2017, 9, 38755-38760.	8.0	204
70	Plasmonic enhanced photoelectrochemical and photocatalytic performances of 1D coaxial Ag@Ag <sub>2</sub> S hybrids. Journal of Materials Chemistry A, 2017, 5, 21570-21578.	10.3	45
71	Trifunctional NiO–Ag–NiO electrodes for ITO-free electrochromic supercapacitors. Journal of Materials Chemistry C, 2017, 5, 8408-8414.	5.5	43
72	Transparent perovskite light-emitting diodes by employing organic-inorganic multilayer transparent top electrodes. Applied Physics Letters, 2017, 111, 213301.	3.3	6

#	Article	IF	CITATIONS
73	Graphene-supported mesoporous titania nanosheets for efficient photodegradation. Journal of Colloid and Interface Science, 2017, 505, 711-718.	9.4	18
74	One-dimensional CdS@MoS2 core-shell nanowires for boosted photocatalytic hydrogen evolution under visible light. Applied Catalysis B: Environmental, 2017, 202, 298-304.	20.2	334
75	Bifunctional MoO <sub>3</sub> –WO <sub>3</sub> /Ag/MoO <sub>3</sub> –WO <sub>3</sub> Films for Efficient ITO–Free Electrochromic Devices. ACS Applied Materials & Interfaces, 2016, 8, 33842-33847.	8.0	56
76	Transparent ambipolar organic thin film transistors based on multilayer transparent source-drain electrodes. Applied Physics Letters, 2016, 109, .	3.3	6
77	Improved Performance of Organic Light-Emitting Field-Effect Transistors by Interfacial Modification of Hole-Transport Layer/Emission Layer: Incorporating Organic Heterojunctions. ACS Applied Materials & amp; Interfaces, 2016, 8, 14063-14070.	8.0	30
78	Near-field dielectric scattering promotes optical absorption by platinum nanoparticles. Nature Photonics, 2016, 10, 473-482.	31.4	298
79	A new hybrid reliability index definition and its application to the structure buckling reliability analysis of supercavitating projectiles. Journal of Shanghai Jiaotong University (Science), 2016, 21, 467-471.	0.9	0
80	Multifarious roles of carbon quantum dots in heterogeneous photocatalysis. Journal of Energy Chemistry, 2016, 25, 927-935.	12.9	127
81	Insight into the Origin of Boosted Photosensitive Efficiency of Graphene from the Cooperative Experiment and Theory Study. Journal of Physical Chemistry C, 2016, 120, 27091-27103.	3.1	37
82	Dual-Functional WO <sub>3</sub> Nanocolumns with Broadband Antireflective and High-Performance Flexible Electrochromic Properties. ACS Applied Materials & Interfaces, 2016, 8, 27107-27114.	8.0	61
83	Black-colored ZnO nanowires with enhanced photocatalytic hydrogen evolution. Nanotechnology, 2016, 27, 22LT01.	2.6	15
84	Efficient Perovskite Solar Cells Based on Multilayer Transparent Electrodes through Morphology Control. Journal of Physical Chemistry C, 2016, 120, 26703-26709.	3.1	12
85	Vertically aligned ZnO–Au@CdS core–shell nanorod arrays as an all-solid-state vectorial Z-scheme system for photocatalytic application. Journal of Materials Chemistry A, 2016, 4, 18804-18814.	10.3	122
86	Structural diversity of graphene materials and their multifarious roles in heterogeneous photocatalysis. Nano Today, 2016, 11, 351-372.	11.9	283
87	Solar–Chemical Energy Conversion by Photocatalysis. Green Chemistry and Sustainable Technology, 2016, , 249-282.	0.7	1
88	The endeavour to advance graphene–semiconductor composite-based photocatalysis. CrystEngComm, 2016, 18, 24-37.	2.6	89
89	Random lasing realized in n-ZnO/p-MgZnO core–shell nanowire heterostructures. CrystEngComm, 2015, 17, 3917-3922.	2.6	13
90	Highly Conductive Transparent Organic Electrodes with Multilayer Structures for Rigid and Flexible Optoelectronics. Scientific Reports, 2015, 5, 10569.	3.3	77

#	Article	IF	CITATIONS
91	Two-Dimensional MoS <sub>2</sub> Nanosheet-Coated Bi <sub>2</sub> S <sub>3</sub> Discoids: Synthesis, Formation Mechanism, and Photocatalytic Application. Langmuir, 2015, 31, 4314-4322.	3.5	178
92	Promoting Visibleâ€Light Photocatalysis with Palladium Species as Cocatalyst. ChemCatChem, 2015, 7, 2047-2054.	3.7	24
93	One-dimensional CdS nanowires–CeO <sub>2</sub> nanoparticles composites with boosted photocatalytic activity. New Journal of Chemistry, 2015, 39, 6756-6764.	2.8	43
94	Silver nanowire/polyimide composite transparent electrodes for reliable flexible polymer solar cells operating at high and ultra-low temperature. RSC Advances, 2015, 5, 24953-24959.	3.6	27
95	Commercialization of graphene-based technologies: a critical insight. Chemical Communications, 2015, 51, 7090-7095.	4.1	74
96	Precursor chemistry matters in boosting photoredox activity of graphene/semiconductor composites. Nanoscale, 2015, 7, 18062-18070.	5.6	67
97	Low-Work-Function, ITO-Free Transparent Cathodes for Inverted Polymer Solar Cells. ACS Applied Materials & Interfaces, 2015, 7, 19960-19965.	8.0	21
98	Waltzing with the Versatile Platform of Graphene to Synthesize Composite Photocatalysts. Chemical Reviews, 2015, 115, 10307-10377.	47.7	1,017
99	Hierarchically CdS Decorated 1D ZnO Nanorodsâ€⊋D Graphene Hybrids: Low Temperature Synthesis and Enhanced Photocatalytic Performance. Advanced Functional Materials, 2015, 25, 221-229.	14.9	394
100	New insight into the enhanced visible light photocatalytic activity over boron-doped reduced graphene oxide. Nanoscale, 2015, 7, 7030-7034.	5.6	62
101	Enhancing the visible light photocatalytic performance of ternary CdS–(graphene–Pd) nanocomposites via a facile interfacial mediator and co-catalyst strategy. Journal of Materials Chemistry A, 2014, 2, 19156-19166.	10.3	130
102	In situ synthesis of hierarchical In <sub>2</sub> S <sub>3</sub> –graphene nanocomposite photocatalyst for selective oxidation. RSC Advances, 2014, 4, 64484-64493.	3.6	28
103	Toward Improving the Graphene–Semiconductor Composite Photoactivity <i>via</i> the Addition of Metal Ions as Generic Interfacial Mediator. ACS Nano, 2014, 8, 623-633.	14.6	352
104	Nanocomposites of graphene-CdS as photoactive and reusable catalysts for visible-light-induced selective reduction process. Journal of Energy Chemistry, 2014, 23, 145-155.	12.9	23
105	Core–Shell Structured Nanocomposites for Photocatalytic Selective Organic Transformations. Particle and Particle Systems Characterization, 2014, 31, 540-556.	2.3	51
106	Toward the enhanced photoactivity and photostability of ZnO nanospheres via intimate surface coating with reduced graphene oxide. Journal of Materials Chemistry A, 2014, 2, 9380.	10.3	204
107	Nanochemistry-derived Bi <sub>2</sub> WO <sub>6</sub> nanostructures: towards production of sustainable chemicals and fuels induced by visible light. Chemical Society Reviews, 2014, 43, 5276-5287.	38.1	368
108	Artificial photosynthesis over graphene–semiconductor composites. Are we getting better?. Chemical Society Reviews, 2014, 43, 8240-8254.	38.1	534

#	Article	IF	CITATIONS
109	Observing the Role of Graphene in Boosting the Two-Electron Reduction of Oxygen in Graphene–WO <sub>3</sub> Nanorod Photocatalysts. Langmuir, 2014, 30, 5574-5584.	3.5	192
110	Graphene Oxide as a Surfactant and Support for In-Situ Synthesis of Au–Pd Nanoalloys with Improved Visible Light Photocatalytic Activity. Journal of Physical Chemistry C, 2014, 118, 5299-5308.	3.1	97
111	A simple yet efficient visible-light-driven CdS nanowires-carbon nanotube 1D–1D nanocomposite photocatalyst. Journal of Catalysis, 2014, 309, 146-155.	6.2	161
112	A Unique Silk Mat-Like Structured Pd/CeO <sub>2</sub> as an Efficient Visible Light Photocatalyst for Green Organic Transformation in Water. ACS Sustainable Chemistry and Engineering, 2013, 1, 1258-1266.	6.7	74
113	A facile one-step way to anchor noble metal (Au, Ag, Pd) nanoparticles on a reduced graphene oxide mat with catalytic activity for selective reduction of nitroaromatic compounds. CrystEngComm, 2013, 15, 6819.	2.6	168
114	Inhibiting Pd nanoparticle aggregation and improving catalytic performance using one-dimensional CeO2 nanotubes as support. Chinese Journal of Catalysis, 2013, 34, 1123-1127.	14.0	13
115	A critical and benchmark comparison on graphene-, carbon nanotube-, and fullerene-semiconductor nanocomposites as visible light photocatalysts for selective oxidation. Journal of Catalysis, 2013, 299, 210-221.	6.2	166
116	Selective oxidation of benzyl alcohol over TiO2 nanosheets with exposed {001} facets: Catalyst deactivation and regeneration. Applied Catalysis A: General, 2013, 453, 181-187.	4.3	97
117	Synthesis of Fullerene–, Carbon Nanotube–, and Graphene–TiO <sub>2</sub> Nanocomposite Photocatalysts for Selective Oxidation: A Comparative Study. ACS Applied Materials & Interfaces, 2013, 5, 1156-1164.	8.0	340
118	Identification of Bi2WO6 as a highly selective visible-light photocatalyst toward oxidation of glycerol to dihydroxyacetone in water. Chemical Science, 2013, 4, 1820.	7.4	313
119	An Efficient Self-Assembly of CdS Nanowires–Reduced Graphene Oxide Nanocomposites for Selective Reduction of Nitro Organics under Visible Light Irradiation. Journal of Physical Chemistry C, 2013, 117, 8251-8261.	3.1	186
120	CdS–graphene nanocomposites as visible light photocatalyst for redox reactions in water: A green route for selective transformation and environmental remediation. Journal of Catalysis, 2013, 303, 60-69.	6.2	202
121	Defective TiO2 with oxygen vacancies: synthesis, properties and photocatalytic applications. Nanoscale, 2013, 5, 3601.	5.6	1,727
122	Synthesis of graphene–ZnO nanorod nanocomposites with improved photoactivity and anti-photocorrosion. CrystEngComm, 2013, 15, 3022.	2.6	309
123	Aggregation- and Leaching-Resistant, Reusable, and Multifunctional Pd@CeO <sub>2</sub> as a Robust Nanocatalyst Achieved by a Hollow Core–Shell Strategy. Chemistry of Materials, 2013, 25, 1979-1988.	6.7	230
124	Transparent organic thin film transistors with WO3/Ag/WO3 source-drain electrodes fabricated by thermal evaporation. Applied Physics Letters, 2013, 103, 033301.	3.3	35
125	Visible-Light-Driven Oxidation of Primary C–H Bonds over CdS with Dual Co-catalysts Graphene and TiO2. Scientific Reports, 2013, 3, 3314.	3.3	116
126	Progress on Graphene-Based Composite Photocatalysts for Selective Organic Synthesis. Current Organic Chemistry, 2013, 17, 2503-2515.	1.6	28

#	Article	IF	CITATIONS
127	Graphene Transforms Wide Band Gap ZnS to a Visible Light Photocatalyst. The New Role of Graphene as a Macromolecular Photosensitizer. ACS Nano, 2012, 6, 9777-9789.	14.6	642
128	Constructing Ternary CdS–Graphene–TiO <sub>2</sub> Hybrids on the Flatland of Graphene Oxide with Enhanced Visible-Light Photoactivity for Selective Transformation. Journal of Physical Chemistry C, 2012, 116, 18023-18031.	3.1	306
129	Synthesis of One-Dimensional CdS@TiO <sub>2</sub> Core–Shell Nanocomposites Photocatalyst for Selective Redox: The Dual Role of TiO <sub>2</sub> Shell. ACS Applied Materials & Interfaces, 2012, 4, 6378-6385.	8.0	345
130	Fabrication of coenocytic Pd@CdS nanocomposite as a visible light photocatalyst for selective transformation under mild conditions. Journal of Materials Chemistry, 2012, 22, 5042.	6.7	139
131	Co2P nanostructures by thermal decomposition: phase formation and magnetic properties. CrystEngComm, 2012, 14, 1197-1200.	2.6	10
132	Recent progress on graphene-based photocatalysts: current status and future perspectives. Nanoscale, 2012, 4, 5792.	5.6	883
133	Recent progress on metal core@semiconductor shell nanocomposites as a promising type of photocatalyst. Nanoscale, 2012, 4, 2227.	5.6	380
134	Transforming CdS into an efficient visible light photocatalyst for selective oxidation of saturated primary C–H bonds under ambient conditions. Chemical Science, 2012, 3, 2812.	7.4	229
135	Improving the photocatalytic performance of graphene–TiO2 nanocomposites via a combined strategy of decreasing defects of graphene and increasing interfacial contact. Physical Chemistry Chemical Physics, 2012, 14, 9167.	2.8	277
136	Emission characteristics of surface second-order metal grating distributed feedback semiconductor lasers. Science Bulletin, 2012, 57, 2083-2086.	1.7	5
137	A Simple Strategy for Fabrication of "Plum-Pudding―Type Pd@CeO <sub>2</sub> Semiconductor Nanocomposite as a Visible-Light-Driven Photocatalyst for Selective Oxidation. Journal of Physical Chemistry C, 2011, 115, 22901-22909.	3.1	121
138	A facile and green approach to synthesize Pt@CeO2 nanocomposite with tunable core-shell and yolk-shell structure and its application as a visible light photocatalyst. Journal of Materials Chemistry, 2011, 21, 8152.	6.7	218
139	LOS rate reconstruction and application of roll-pitch seeker. , 2011, , .		0
140	Assembly of CdS Nanoparticles on the Two-Dimensional Graphene Scaffold as Visible-Light-Driven Photocatalyst for Selective Organic Transformation under Ambient Conditions. Journal of Physical Chemistry C, 2011, 115, 23501-23511.	3.1	333
141	Synthesis of M@TiO <sub>2</sub> (M = Au, Pd, Pt) Core–Shell Nanocomposites with Tunable Photoreactivity. Journal of Physical Chemistry C, 2011, 115, 9136-9145.	3.1	558
142	Research on the effect of clamp on rudder lift-drag characteristics. , 2011, , .		0
143	Image parallel processing based on GPU. , 2010, , .		39